Malaysian NANO-An International Journal

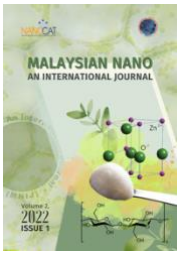

Research Article

The synergistic effect of N-doped TiO_2-SiO_2 nanocatalysts and peroxydisulfate towards improving Bisphenol A photodegradation efficiency

T.V. Nguyen[a,b], P.N.M. Le[a,b], N.D.T. Huynh[a,b], T.H. Ngo[a,b], H.T. Huynh[a,b] , M.V. Le[a,b*]

[a] *Faculty of Chemical Engineering, Ho Chi Minh City University of Technology (HCMUT),268 Ly Thuong Kiet Street, District 10, Ho Chi Minh City 700000, Vietnam.*

[b] *Vietnam National University Ho Chi Minh City, Linh Trung Ward, Thu Duc District, Ho Chi Minh City 700000, Vietnam.*

Received July 5, 2022
Revised July 30, 2022
Accepted August 2, 2022

DOI:
https://doi.org/10.22452/mnij.vol2no1.2

Corresponding authors:
lmvien@hcmut.edu.vn

Abstract

TiO_2-based photocatalysts have attracted tremendous attention for the degradation of hazardous organic pollutants in sewage. In this work, a series of N-doped TiO_2-SiO_2 with varying N contents (10N-TS5, 20N-TS5, 30N-TS5) were successfully synthesized via sol-gel method. The physical properties of the catalyst are characterized using X-ray diffraction (XRD), scanning electron microscopy (SEM), energy dispersive emission spectroscopy (EDX), UV-visible absorption spectroscopy, and specific surface area (BET) measurements. The photocatalytic activities of as-prepared catalysts were assessed by degrading 10 mg. L^{-1} Bisphenol A (BPA) under simulated natural light irradiation. The results indicate that the N doping in the TiO_2-SiO_2 nanostructures can reduce the crystal sizes, improve the BET surface areas, and narrow the band gap energy, thereby enhancing the photocatalytic activity of the materials. The 10N-TS5 exhibits the best photoactivity, which degrades 90.7 % of BPA for 240 min irradiation. Noteworthy, the presence of 2 mM peroxydisulfate (PDS, $S_2O_8^{2-}$) in the 10N-TS5 reaction system removes completely 10ppm BPA for only 50 min illumination with the rate constant of 10.9×10^{-2} min^{-1}, 7.8 times higher than that of 10N-TS5 suspension without PDS agent. The N-doped TiO_2-SiO_2 photocatalyst coupling with PDS provides a promising pathway for environmental remediation.

Keywords*:* N doped TiO_2-SiO_2; Nanocatalyst; Bisphenol A; photodegradation; peroxydisulfate.

1. Introduction

In recent years, advanced oxidation processes (AOP) using heterogeneous photocatalysts have been shown to be an effective technique for eliminating hazardous pollutants. In particular, titanium dioxide (TiO_2) is considered a typical material that is used widely in wastewater treatment due to its outstanding properties such as high oxidative capacity, low cost, mechanical and chemical stability, and environmental friendliness [1-3]. However, to further use in practical applications, it is necessary to modify the pristine TiO_2 in which the specific surface area and the visible light absorption are improved.

Numerous researches have suggested that the combination of TiO_2 semiconductor and porous materials with high specific surface area (e.g. SiO_2, Al_2O_3) to form nanocomposites can enlarge BET surface area [4-6]. Among them, amorphous silica (SiO_2) introduced into the TiO_2 lattices is reported not only to improve the adsorption capability of TiO_2 based on the specific surface area improvement, but also to suppress electron-hole recombination rate, hinder crystal growth and anatase-rutile phase transformation, leading to promote the photocatalytic activity [7]. Nevertheless, the presence of SiO_2 in TiO_2-SiO_2 composites causes the blue shift of the wavelength absorption due to the band-gap broadening, thus limiting the effectiveness of the catalyst in the visible light region [8].

To overcome this challenge, elemental doping, especially non-metal doping is one of the effective approaches which are proposed to upgrade the optical properties of TiO_2-SiO_2 composites. Therein, the non-metallic element N is the most widely utilized element because it is close to the O element in both atomic radius and elemental position, and some of the O atoms can be substituted by N atoms [9]. The N-doped TiO_2-SiO_2 composites are proven to have good activity in degrading effectively many types of pollutants such as azo dyes [9], antibiotics [10], aromatics[11], etc. Consequently, N-doped TiO_2-SiO_2 is a potential candidate drawing great deal of concern for removing contaminants in polluted water.

Recently, sulfate radicals (SR, $SO_4^{\bullet-}$) derived from the activation of PDS by TiO_2-based photocatalyst exhibit superior decontamination prospects than hydroxyl radicals, which is attributed to the higher redox potential, longer half-life as well as their formation in a broader pH range [12]. Pollutants are degraded very rapidly when the reaction system is present with both photocatalyst and PDS due to their mechanism of synergistic effect for creating many radical species such as $SO_4^{\bullet-}$, $OH^{\bullet}$, $O_2^{-\bullet}$ [13-16]. Therefore, the involvement of PDS into photodegradation processes is a simple and useful strategy for boosting the performance of catalysts.

In this study, we focused on exploring the influences of the dopant amount of N on the photocatalytic activity of N-doped TiO_2-SiO_2 composites synthesized via sol-gel method. Various analytical techniques were employed to characterize the physicochemical properties of prepared materials. The activities of composites were evaluated through the degradation of BPA under simulated natural light. Furthermore, the effect of PDS concentrations on the BPA degradation rates was also investigated. Radical scavenging experiments were conducted to identify the radical species dominating the BPA oxidation.

2. Materials and Methods

2.1. Reagents and chemicals.

All the chemicals were used as purchased without further purification. Titanium IV butoxide (TNB, $Ti(OC_4H_9)_4$, > 97%) and tetraetyl orthosilicat (TEOS, $SiC_8H_{20}O_4$, > 98%) were used as precursors of TiO_2 and SiO_2 nanoparticles and both were purchased from Sigma Aldrich. Urea (CH_4N_2O, 99%) manufactured by Merck was used as the N-dopant precursor. Polyethylene glycol 2000 (PEG, Sigma Aldrich), ethanol (99.5%, COMECO), acetyl acetone (AcAc, $C_5H_8O_2$, HIMEDIA, > 99%), and acid nitric (HNO_3, 65%, Merck) were used for catalysts synthesis.

2.2. Catalyst preparation

N-doped-TiO_2-SiO_2 (Ti/Si molar ratio was 95:5) composite was fabricated using facile sol-gel method. Ethanol was used as a solvent for both N-dopant and titania precursors. Different amounts of urea (1:10, 2:10 and 3:10, N: Ti molar ratio) were dissolved in 5 mL ethanol. The above mixture was then added to the solution containing 4 g TNB. After 15 mins under stirring in order to well-disperse, 1.2 mL AcAc and 0.5mL HNO_3 65% were added to form solution A. Solution A was kept at 80°C under magnetic for 1 h to form homogeneous solution. Solution B included 0.129 g TEOS, 0.2 g PEG-20000, 5 mL ethanol, 0.5 mL HNO_3 65%, and 2.4 mL deionized water was also mixed under vigorgous stiring at ambient condition. After 1 h stirring, solution A was dropwise added into solution B and continuously stirring for 2 h to sol then aged at room temperature for 2 days. The resulting mixture was allowed to dry at 120 °C until the solvent was completely removed before being calcined at 500 °C for 2 h in air at a heat rate of 2 °C.min^{-1}. To obtain the final powders, the collected dry powder was balling crushed in ethanol solvent for 8 h before being dried at 120 °C. The obtained powders were denoted as xN-TS5 while "x" ascribed to the N-dopant and titania molar ratio. The bare TiO_2-SiO_2 (TS5) catalyst was prepared via the same procedure without the addition of urea.

2.3. *Material characterization*

X-ray diffraction patterns were collected using Cu-Kα (λ = 0.154184 nm) as the Brucker machine's radiation source (Lynxeye detector, D2 phaser, Germany) with diffraction angle (2θ) scanned from 20 ° to 80 °. Morphological characterization and the chemical composition were detected using SEM (Hitachi Fe-SEM S4800) equipped with the EDX spectroscopy (EX 350-Horiba). UV-Vis absorbance spectra of the photocatalysts was measured on JASCO V-550 with the scanning wavelength in the range of 250 – 800 nm. The BET surface area and Dubinin-Astakhov (DA) pore size distribution in nitrogen adsorption isotherm were determined by Quantachrome NOVA 1000E Surface Area and Pore Size analyzer at 77K.

2.4. *Photocatalytic degradation of Bisphenol-A*

Throughout this study, the catalytic performance was tested against BPA as the representative organic contaminant. The photocatalytic activity testing experiments were conducted according to previous reported research [17]. In detail, a 26 W Exo Terra Natural Light with a wavelength from 290 to 740 nm was used as a simulated natural light source. The process of photodegradation was carried out at ambient temperature as follows: 0.2 g of photocatalyst was added into an aqueous solution of 10 mg. L^{-1} BPA. Then the suspension was magnetically stirred for 60 min in dark to reach the adsorption – desorption equilibrium. After the lamp was turned on, at a given time intervals of irradiation, 5 mL mixture was taken from the suspension and filtered through 0.45 μm nylon filter and analyzed the remained BPA concentration by UV-Vis HITACHI U-2910 spectrometer at the wavelength of 225 nm. For the photocatalytic activation of peroxydisulfate, the desired amounts of peroxydisulfate (0.25, 0.5, 1, 2, 3 mM) were added into suspension after 60 min stirring in dark.

Trapping experiments were performed to study the main effective reactive species in the BPA degradation by N-doped-TiO_2-SiO_2 composite. For peroxydisulfate-mediated reactions, ethanol (EtOH, 1 M) and isopropanol (IPA, 1 M) were usually used as quenching agents for both $SO_4^{\bullet-}$, and $OH^{\bullet}$. Nitrogen gas (N_2) was purged into the suspension for 15 min before turning on the lamp to inhibit the generation of $O_2^{-\bullet}$ reactive species.

3. Results and discussion

3.1. *Characterization of prepared photocatalysts*

The crystal phase of the TiO_2-SiO_2 composite and N-doped photocatalysts were characterized by XRD and the results are displayed in Figure 1. Diffraction peaks of sample at 25.3°, 37.8°, 48.2°, 54.8°, 63.0°, 69.5°, 75.1° are in turn assigned to the crystal planes (101), (004), (200), (211), (204),

(220) and (215) of TiO_2 anatase phase (JCPDS Card No. 21-1272). In addition, the absence of rutile peaks indicates that the crystalline phase of the nanoparticles was pure anatase and no diffraction peaks of SiO_2 were observed, confirming that SiO_2 was formed in the amorphous phase. Other phases evidence was not observed considering the suppression of TiO_2 anatase – rutile transformation by adding the silica agent. There was no specific peak detected in the N-doping samples, which implies that the dopants do not change the crystal structure. The crystallite size of the nanocatalysts was calculated by using Debye - Scherrer equation with the data extracted at (101) reflections of anatase phase, as shown in Table 1. With the N doping, TS5 nanocomposite reduced its crystallite size due to the Ti-O-Si and Ti-O-S bond formation to block grain growth [18].

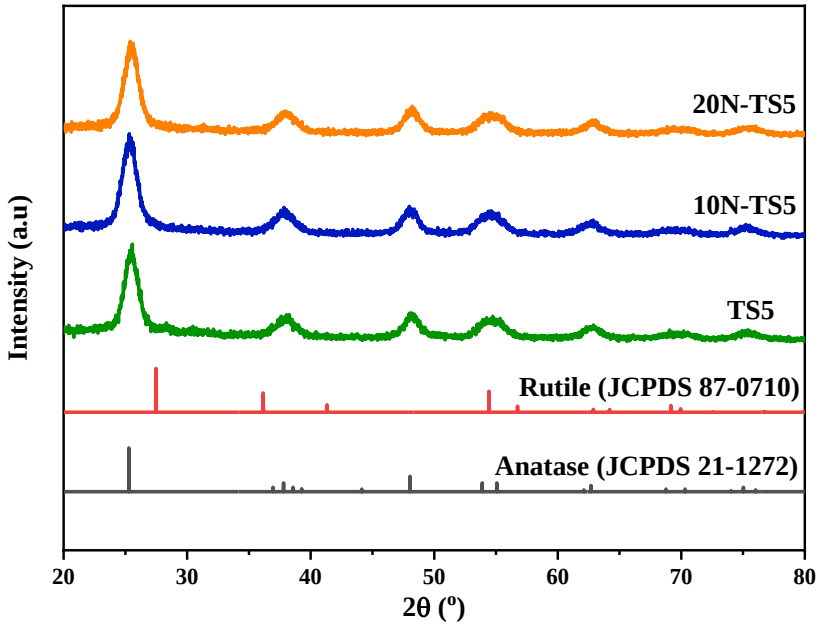

Figure 1: XRD patterns of TS5, 10N-TS5, and 20N-TS5

Table 1: Detail characterization of TS5 and N-TS5 with two different concentration of N dopant according to XRD analysis

Sample	2θ (101)	FWHM – β (101)	Crystallite size (nm)
TS5	25.48	1.38	5.91
10N-TS5	25.34	1.46	5.58
20N-TS5	25.46	1.48	5.51

The microstructural properties of samples were investigated using N_2 adsorption – desorption isotherms at 77 K. Figure 2 shows the adsorption – desorption isotherms and Dubinin-Astakhov pore size distribution from the adsorption profiles of TS5 and 10N-TS5. TS5 displayed a type IV isotherm with H3 hysteresis loop as with 10N-TS5, indicating the presence of typical slit-shape mesoporous. Compare with TS5, the BET surface area, average diameter, and mesoporous volume of 10N-TS5 is improved remarkably by introducing N-dopant into the TS5 lattice (Table 2). Pore volume of 10N-TS5 was 1.5 times larger than that of pure TS5 and the BET specific surface area of TS5 was moderately increased when doping with N. The enhancement in BET surface area, mesopore volume, and pore diameter are conducive to expose more accessible active sites and improve the mass transfer efficiency, thereby accelerating the catalytic role.

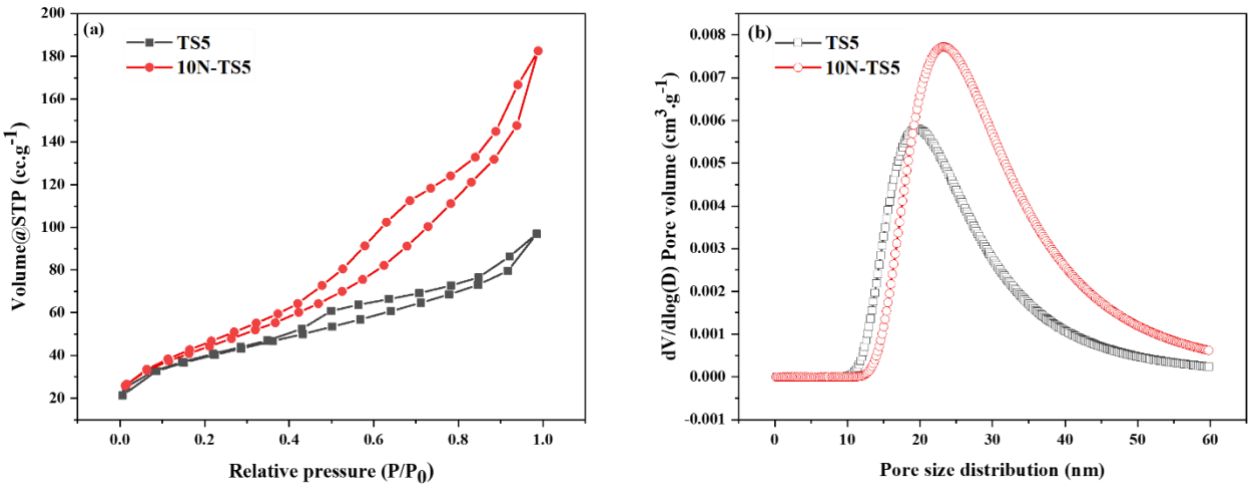

Figure 2: N_2 adsorption-desorption isotherms (a); Micropore size distribution by the Dubinin-Astakhov method (b) of the as-prepared TS5 and 10N-TS5

Table 2: BET specific surface area (S_{BET}), average pore diameter (D_{BET}), and total pore volume for TS5 and 10N-TS5

Sample	BET surface area ($m^2.g^{-1}$)	Pore volume ($cm^3.g^{-1}$)	Average pore diameter (nm)
TS5	136.27	0.11	1.96
10N-TS5	156.97	0.17	2.32

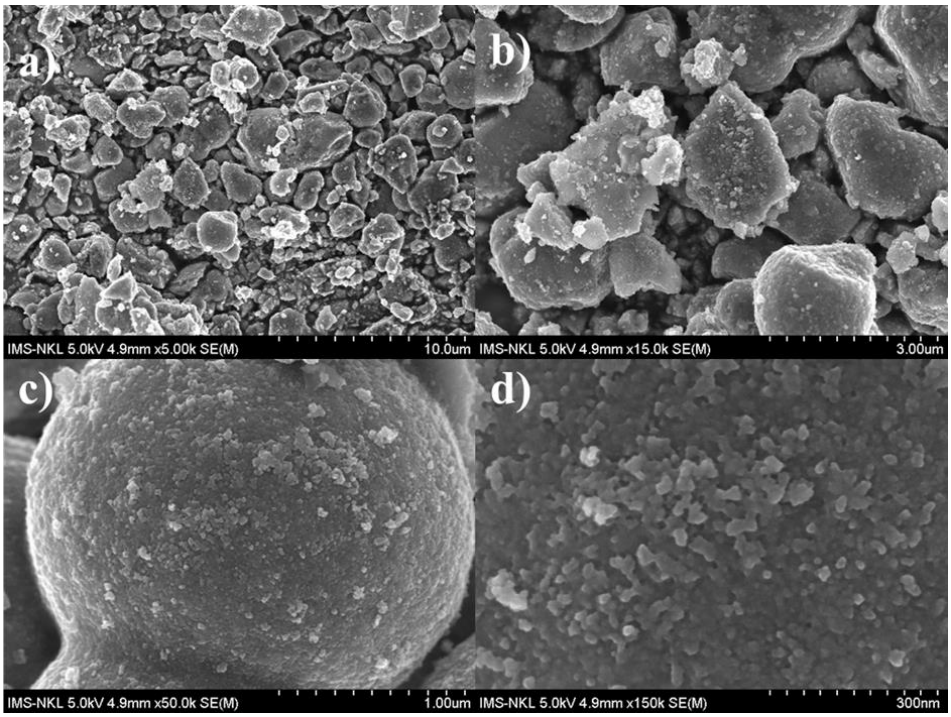

Figure 3: FE-SEM images of 10N-TS5 at different magnifications

The morphology of 10N-TS5 powder was observed by FE-SEM images (Figure 3). The 10N-TS5 sample comprised fractal particles with the uneven size distribution. The sample also occurred agglomeration. This phenomenon has also been reported in previous studies [7, 19] .

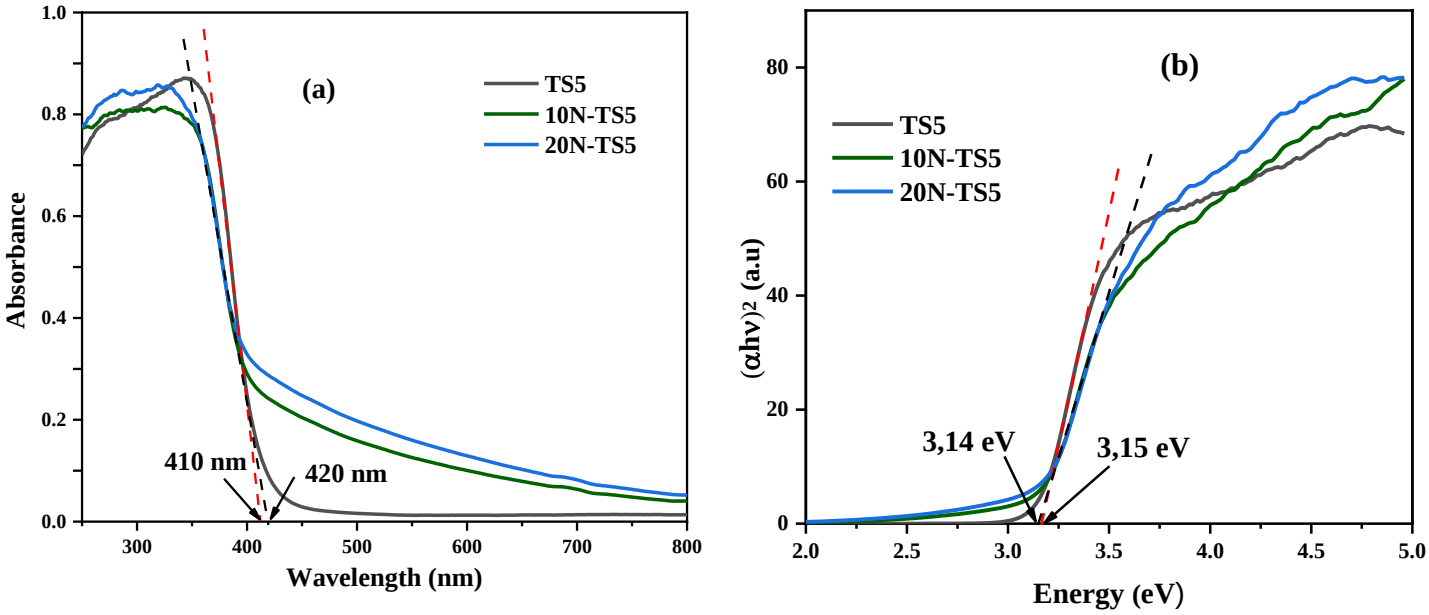

Figure 4 (a): UV-Vis DRS of TS5, 10N-TS5, 20N-TS5 and (b) Tauc plots of TS5, 10N-TS5, 20N-TS5

Figure 4a depicts the light absorption spectra of photocatalysts in the wavelength range of 250 – 800 nm. The light absorption of the N-doped TiO_2-SiO_2 composites in the visible light range is clearly increased, which may be ascribed to the creation of a localized intermediate band gap N 2p energy level in the O 2p valence band of TiO_2 with N element doping. As a result, electrons at this energy level can be driven to the TiO_2 conduction band, allowing photons with longer wavelengths to be absorbed as well, making the optical response of TiO_2 red-shifted and improving the absorption ability in visible light [9].

The band gap energy of each sample was calculated based on the UV–vis data using the Tauc plot method as shown in Figure 4b. The 10N-TS5 and 20N-TS5 samples exhibit the same band gap energy of 3.14 eV, slightly reduce in comparison with pristine TS5 composite (3.15 eV), which again shows that the doping of N element broadens the light response range of the samples.

3.2. Effect of N-dopant concentration on the degradation of BPA

The performance of the four different nanocomposite photocatalyst materials was investigated in the photodecomposition of Bisphenol-A (BPA) under simulated natural light irradiation. Figure shows the trend observed in the removal of BPA. Under light irradiation, the pure TS5 composite performed a rather good catalytic activity, whose degradation efficiency was 82 % after 240 min irradiation. It was observed that the effect of TiO_2-SiO_2 composite was better when doping with N-dopant. There was marked improvement in the rate of photocatalytic breakdown of BPA in the visible range. For the N-TS5 series photocatalyst, the order of kinetic rate is: 10N-TS5 > 20N-TS5 > 30N-TS5. The degradation efficiency of 10N-TS5 reached 90 % after 240 min under simulated natural light irradiation and its pseudo-first-order kinetic rate was 1.5 times higher than that of TS5, which should be attributed to the high electron mobility of N inducing the effective separation of electron – hole pairs. The good photocatalytic activity for N-TiO_2-SiO_2 at visible illumination is not strongly related to the enhancement in light absorption, but due to the occupation of N on O lattice site leads to the formation of the donor level. With the deep trapped of donor level, the photo-induced electrons - holes are separated. The catalytic efficiency exhibits a trend of decreasing with the increase of N element doping. This could be referred to the appropriate amount of N incorporation that promotes the effective separation of photo-generated charges, but excessive N elements lead to compounding of photogenerated electrons during the transport process [9].

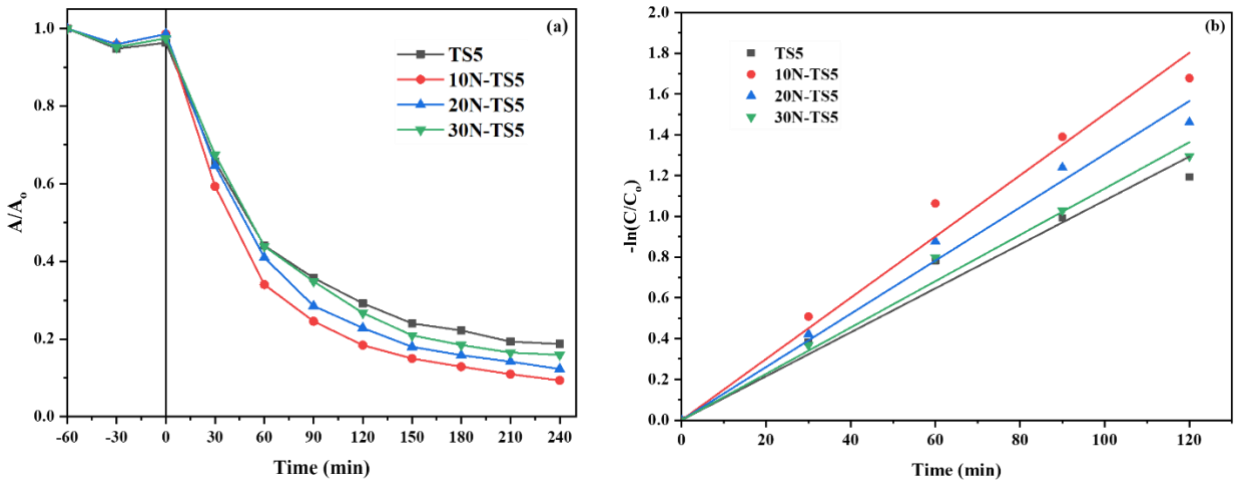

Figure 5: Photocatalytic degradation of BPA using un-doped and doped TS5 samples: (a) photocatalytic degradation efficiency and (b) first-pseudo degradation kinetics

3.3. Effect of peroxydisulfate concentration

Another possibility to inhibit electron – hole pairs recombination is the use of peroxydisulfate as an electron acceptor. To further evaluate the peroxydisulfate activating ability of 10N-TS5, BPA removal efficiency in the 10N-TS5/PDS with different amounts of PDS added (0.25, 0.5, 1, 2, 3 mM) has been investigated. The presence of PDS in the photocatalytic reaction can significantly improve the BPA removal efficiency as seen in Figure . There are two potential reasons: (1) more $SO_4^{\bullet -}$ were generated from $S_2O_8^{2-}$ with e^- form by 10N-TS5 when it was induced; (2) the recombination of electron – hole pairs was reduced as the reaction between the electrons and PDS [13]. Therefore, the enhancement of BPA degradation performance may be due to the synergistic function of 10N-TS5 and PDS. When the concentration of PDS increased from 0.25 mM to 2 mM, the degradation efficiency increased from 63 % to 96 % after 30 min irradiation. BPA was completely decomposed after 50 min irradiation by the reaction system of 10N-TS5/ 2 mM PDS. When the PDS concentration was 3 mM, the BPA removal was decreased (76 % after 30 min irradiation). This debasement in removal rate is considering the quenching of hydroxyl and sulfate radicals. Furthermore, by raising the PDS concentration, the reaction between radicals with others increased, lessening the availability of these radicals in solution.

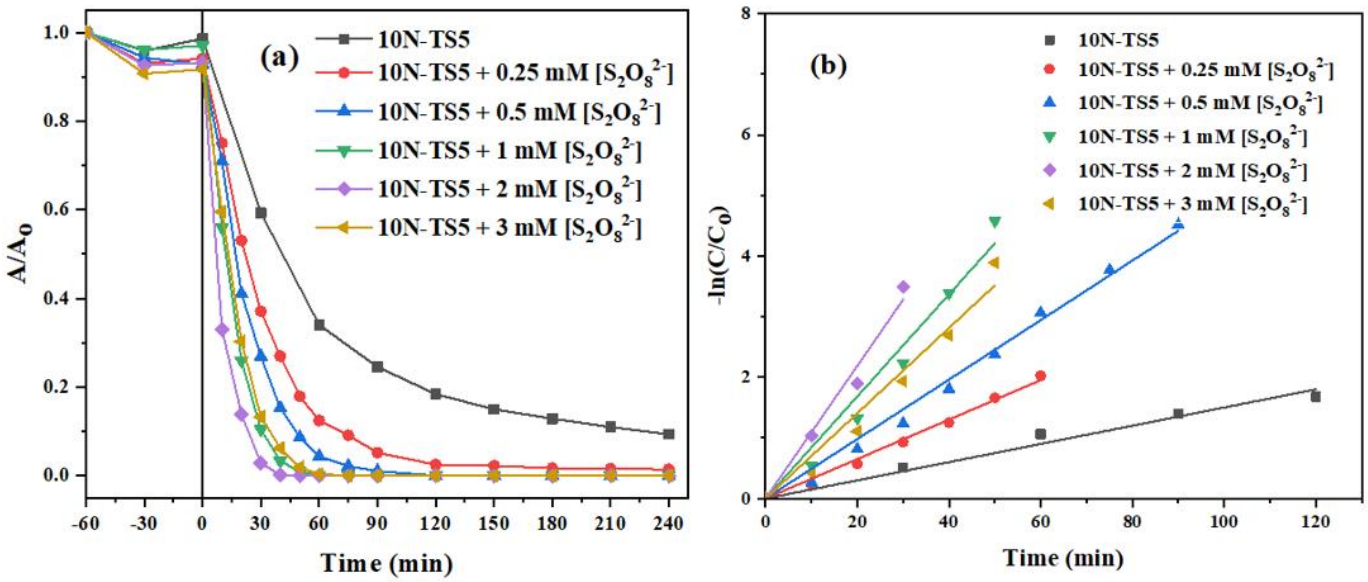

Figure 6: Effect of peroxydisulfate concentrations on the BPA degradation using TS5 and N-TS5 (initial BPA concentration: 10 mg. L^{-1}, catalyst dosage: 1 g.L^{-1})

3.4. Effect of radical scavengers

To further evaluate the role of active radicals in the degradation of BPA assisted by peroxydisulfate ion, free radicals capture experiments have been conducted. In each quenching experiment, the concentration of BPA was 10 mg. L^{-1}, the dosage of 10N-TS5 was 1 g. L^{-1}, and the dose of EtOH and IPA was 1 M. N_2 (nitrogen purity: 99%) was utilized for quenching $O_2^{-\bullet}$. The effect of free reactive species on the BPA photodegradation over 10N-TS5 is depicted in Figure 7. As shown in Table 3, the kinetic rate of BPA oxidation degradation was decreased as the consequence of scavengers. The presence of IPA led to the decline of kinetic rate (from 10.9×10^{-2} to 2.9×10^{-2} min^{-1}), while EtOH further inhibited the reaction rate (1.8×10^{-2} min^{-1}). However, the removal of BPA was drastically quenched by N_2 purging. This observation demonstrates the importance of oxygen to the degradation of BPA as the source of $O_2^{-\bullet}$ species. It was thereby concluded that $SO_4^{\bullet-}$ and $O_2^{-\bullet}$ generated by light-induced electrons were the dominant reactive species for BPA degradation.

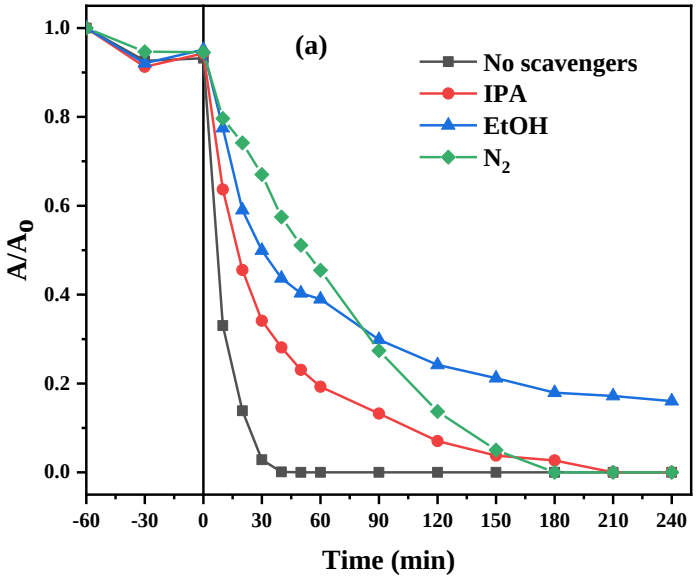

Figure 7: Effect of different scavengers on BPA degradation in the presence of 10N-TS5 photocatalyst under the assistance of peroxydisulfate ion

Table 3: First order reaction kinetic constants and correlation coefficients in peroxydisulfate assisted BPA photocatalytic degradation

Scavengers	Kinetic rate (min^{-1})	R^2
No scavengers	10.9×10^{-2}	0.99
IPA	1.8×10^{-2}	0.99
EtOH	2.9×10^{-2}	0.98
N_2	1.2×10^{-2}	0.99

4. Conclusions

In conclusion, N-doped TiO_2-SiO_2 nanocomposites were successfully synthesized by facile sol-gel method. The crystallite size of 10N-TS5 and 20N-TS5 is both smaller than TS5, showing that the N modification method is very effective in reducing the catalyst particle size. The BET surface area of sample 10N-TS5 is 156.97 $m^2.g^{-1}$, which is larger than that of pristine TS5. All three samples of N doped TS5 possess high activity in BPA degradation, in which the 10N-TS5 shows the highest photodegradation yield of 90.7 % after 240 min of irradiation. Therefore, it can be concluded that N denaturation helps to expand the photon absorption region to the visible region compared with the unmodified TS5 catalyst. Moreover, the integration between 10N-TS5 and PDS increased the degradation rate up to 7.8 times and degraded completely 10 ppm BPA in aqueous for only 50 min of irradiation, much faster than that of the catalyst-only reaction system. This study has proposed a simple and effective method for the removal of persistent pollutants in the aquatic environment.

Acknowledgements

We acknowledge the support of time and facilities from Ho Chi Minh, City University of Technology (HCMUT), VNU-HCM for this study.

Conflicts of interest

The authors declare no conflict of interest.

References

[1] D. Chen *et al.*, "Photocatalytic degradation of organic pollutants using TiO_2-based photocatalysts: A review," *Journal of Cleaner Production.* 2020; 268:121725.

[2] B. Bakbolat *et al.*, "Recent developments of TiO_2-based photocatalysis in the hydrogen evolution and photodegradation: a review," *Nanomaterials.* 2020; 10, 9: 1790.

[3] H. Xu, Z. Hao, W. Feng, T. Wang, and Y. Li, "Mechanism of Photodegradation of Organic Pollutants in Seawater by TiO_2-Based Photocatalysts and Improvement in Their Performance," *ACS omega.* 2021; 6, 45, 30698-30701.

[4] C. G. Joseph, Y. H. Taufiq-Yap, B. Musta, M. S. Sarjadi, and L. Elilarasi, "Application of plasmonic metal nanoparticles in TiO_2-SiO_2 composite as an efficient solar-activated photocatalyst: A review paper," *Frontiers in Chemistry.* 2021; 8: 568063.

[5] U. Mahanta, M. Khandelwal, and A. S. Deshpande, "TiO_2@ SiO_2 nanoparticles for methylene blue removal and photocatalytic degradation under natural sunlight and low-power UV light," *Applied Surface Science* 2022; 576: 151745.

[6] D.-J. Liu, J.-H. Lei, S. Wei, B.-L. Jiang, and Y.-T. Xie, "Degrading methyl orange via prepare high dispersed TiO_2/Al_2O_3 photocatalyst by combining anodizing and hydro-thermal technology," *AIP Advances.* 2022; 12, 7: 075207.

[7] M. Jesus, A. Ferreira, L. Lima, G. Batista, R. Mambrini, and N. Mohallem, "Micro-mesoporous TiO_2/SiO_2 nanocomposites: Sol-gel synthesis, characterization, and enhanced photodegradation of quinoline," *Ceramics International.* 2021; 47,17: 23844-23850.

[8] T.-N.-B. Duong and M.-V. Le, "High efficiency degradation of tetracycline antibiotic with TiO_2-SiO_2 photocatalyst under low power of simulated solar light irradiation," in *AIP Conference Proceedings*. 2019; 2085, 1: 020020.

[9] C. Wu, X. Dong, L. Wang, L. Zhang, and X. Liu, "Preparation of N-TiO_2/SiO_2 composites by solvothermal method and their photocatalytic properties," *Materials Research Express*. 2022;9, 5: 055002.

[10] S. K. Kassahun, Z. Kiflie, H. Kim, A. F. Baye, and Innovation, "Process optimization and kinetics analysis for photocatalytic degradation of emerging contaminant using N-doped TiO_2-SiO_2 nanoparticle: Artificial Neural Network and Surface Response Methodology approach," *Environmental Technology*. 2021;23: 10176.

[11] H.-T. Huynh, M.-V. Le, and L. Van Hoang, "Enhanced photocatalytic degradation of N-doped TiO_2-SiO_2 composite for degradation of phenol under simulated natural light assisted by $S_2O_8^{2-}$ anions," in *IOP Conference Series: Earth and Environmental Science*. 2021; 947, 1: 012020.

[12] Y. Peng, H. Tang, B. Yao, X. Gao, X. Yang, and Y. Zhou, "Activation of peroxymonosulfate (PMS) by spinel ferrite and their composites in degradation of organic pollutants: A Review," *Chemical Engineering Journal*. 2021;414: 128800.

[13] Y. Rao, Y. Zhang, A. Li, T. Zhang, and T. Jiao, "Photocatalytic activity of G-TiO_2@ Fe_3O_4 with persulfate for degradation of alizarin red S under visible light," *Chemosphere*.2021; 266: 129236.

[14] Q. Tang, X. An, H. Lan, H. Liu, and J. Qu, "Polyoxometalates/TiO_2 photocatalysts with engineered facets for enhanced degradation of bisphenol A through persulfate activation," *Applied Catalysis B: Environmental*. 2020; 268: 118394.

[15] M. Sabri, A. Habibi-Yangjeh, H. Chand, and V. Krishnan, "Activation of persulfate by novel TiO_2/FeOCl photocatalyst under visible light: facile synthesis and high photocatalytic performance," *Separation Purification Technology*. 2020; 250; 117268.

[16] Y. Zhang and W. Chu, "Bisphenol S degradation via persulfate activation under UV-LED using mixed catalysts: Synergistic effect of Cu–TiO_2 and Zn–TiO_2 for catalysis," *Chemosphere*. 2022; 286: 131797.

[17] V. Q. T. Hoang, T. Q.-P. Phan, V. Senthilkumar, V. T. Doan, Y. S. Kim, and M. V. Le, "Enhanced photocatalytic activities of vandium and molybdenum co-doped strontium titanate under visible light," *International Journal of Applied Ceramic Technology*. 2019;16, 4: 1651-1658.

[18] X. Chen, H. Sun, J. Zhang, Y. Guo, and D.-H. Kuo, "Cationic S-doped TiO_2/SiO_2 visible-light photocatalyst synthesized by co-hydrolysis method and its application for organic degradation," *Journal of Molecular Liquids*. 2019; 273: 50-57.

[19] G. Lu, X. Wang, Y. Wang, G. Shi, X. Xie, and J. Sun, "Anti-oxidative microstructure design of ultra-stable N-TiO_2 composite for the gaseous photodegradation reactions," *Chemical Engineering Journal.* 2021; 408: 127257.